Biomass combustion with *in situ* CO_2 capture by CaO in a 300 kW_{th} circulating fluidized bed test facility

M. Alonso[a]*, M.E. Diego[a], C Pérez[b], J.R. Chamberlain[b], J.C. Abanades[a]

[a]Spanish Research Council, INCAR-CSIC, C/ Francisco Pintado Fe, 26, 33011 Oviedo, Spain

[b]Gas Natural Fenosa, GNF, Avenida de San Luis 77, Madrid, Spain

*Corresponding author. T.: 34-985119090. E-mail: mac@incar.csic.es

ABSTRACT

This paper reports experimental results from a new 300 kW_{th} calcium looping pilot plant designed to capture CO_2 "in situ" during the combustion of biomass in a fluidized bed. This novel concept relies on the high reactivity of biomass as a fuel, which allows for effective combustion around 700ºC in air at atmospheric pressure. In these conditions, CaO particles fed into the fluidized bed combustor react with the CO_2 generated during biomass combustion, allowing for an effective CO_2 capture. A subsequent step of regeneration of $CaCO_3$ in an oxy-fired calciner is also needed to release a concentrated stream of CO_2. This regeneration step is assumed to be integrated in a large scale oxyfired power plant and/or a larger scale post-combustion calcium looping system.

The combustor-carbonator is the key reactor in this novel concept, and this work presents experimental results from a 300 kW_{th} pilot to test such a reactor. The pilot involves two 12 m height interconnected circulating fluidized bed reactors. Several series of experiments to investigate the combustor-carbonator reactor have been carried out achieving combustion efficiencies close to 100% and CO_2 capture efficiencies between 70-95% in dynamic and stationary state conditions, using wood pellets as a fuel. Different superficial gas velocities, excess air ratios above stoichiometric requirements, and solid circulating rates between combustor-carbonator and combustor-calciner have been tested during the experiments. Closure of the carbon and oxygen balances during the combustion and carbonation trials has been successful. A simple reactor model for combustion and CO_2 capture in the combustor-carbonator has been applied to aid in the interpretation of results, which should facilitate the future scaling up of this process concept.

Keywords: Biomass combustion, CO2 capture, negative emissions, calcium looping, BECCS.

INTRODUCTION

Calcium looping, CaL, or "carbonate looping" embraces a range of CO_2 capture technologies where CaO is used as a regenerable sorbent of CO_2. During the CO_2 absorption step at atmospheric pressure, the carbonation reaction of CaO with CO_2 at temperatures between 600-750 ºC takes place. During the regeneration step, calcination of $CaCO_3$ at temperatures above 870ºC in a rich atmosphere of CO_2 is achieved by oxyfuel combustion of an additional fuel in the calciner. Several recent reviews (Blamey et al., 2010; Anthony, 2011; Abanades, 2013; Boot-Handford et al., 2014) have highlighted the theoretical benefits of this technology that arise from the possibility to efficiently recover the energy used for sorbent regeneration.

The CaL technology is being rapidly scaled up as a post-combustion CO_2 capture system because of the similarity of the key reactors (carbonator and calciner) with those in existing power plants using circulating fluidized bed combustors, CFBCs. The post-combustion process scheme was early proposed by Shimizu et al. (Shimizu et al., 1999) and further developed in the early 2000s at laboratory and bench scales in our group (Abanades, 2002; Abanades and Alvarez, 2003; Abanades et al., 2004). This was followed by the publication of results from several lab scale fluidized bed pilots (10s kW_{th}) involving continuous solid circulation (Alonso et al., 2010; Charitos et al., 2010; Charitos et al., 2011; Rodriguez et al., 2011a). More recently, steady state results have been reported from 0.2 MW_{th} pilot located in Stuttgart University (Hawthorne et al., 2010; Dieter et al., 2014) and a 1 MW_{th} pilot in Darmstadt (Galloy et al., 2011; Ströhle et al., 2014; Plötz et al., 2012). Other large scale pilots are being built in Taiwan (Chang et al., 2013). The largest Calcium looping pilot (1.7 MW_{th}) successfully operated in post-combustion mode is located in La Pereda CFBC power plant (Spain) and has recently reported several hundreds of hours of steady state results treating 1/150 th of the flue gases of the existing coal power plant and achieving continuous calcination of $CaCO_3$ by oxy-combustion of coal in a CFBC (Sánchez-Biezma et al., 2012; Arias et al., 2013).

In this work we deal with a particular process variant of a Calcium looping system that intends to exploit the high temperature $CaO/CaCO_3$ chemical loop to achieve the effective capture of CO_2 "in situ" during the combustion of biomass in a fluidized bed boiler (Abanades et al., 2011a). The use of biomass as a fuel in CCS systems (Bio-CCS or BECCS) leads to processes with negative emissions of CO_2 (Ishitani and Johansson, 1996; Obersteiner et al., 2001; Rhodes and Keith, 2008). BECCS technologies may need to be deployed to meet the lowest targets of atmospheric CO_2 concentration (Koornneef et al., 2012; IPCC, 2014) as these technologies are the only option to reverse historical emissions of CO_2.

The schematic concept of the particular Calcium Looping process considered in this work is represented in Figure 1. It includes two interconnected circulating fluidized bed

combustors ($CFBC_S$). One of the $CFBC_s$ is operating at modest combustion temperatures (700ºC) to allow for simultaneous CO_2 capture by carbonation of CaO (the equilibrium partial pressure of CO_2 on CaO at atmospheric pressure is just 3.0 vol% at 700ºC). The $CaCO_3$ formed in this CFB combustor-carbonator reactor circulates to the second CFBC operated in oxyfuel combustion mode at a typical biomass combustion temperature range (840-900 ºC) (Saidur et al., 2011), where the CO_2 is released and the CaO regenerated to circulate back to the CFB combustor-carbonator. The concept has been already demonstrated by our group in a 30 kW_{th} test facility over a range of operating conditions (Alonso et al., 2011). Overall CO_2 capture efficiencies higher than 80 % were achieved with sufficiently high solids circulation rates of CaO and solids inventories in the combustor-carbonator.

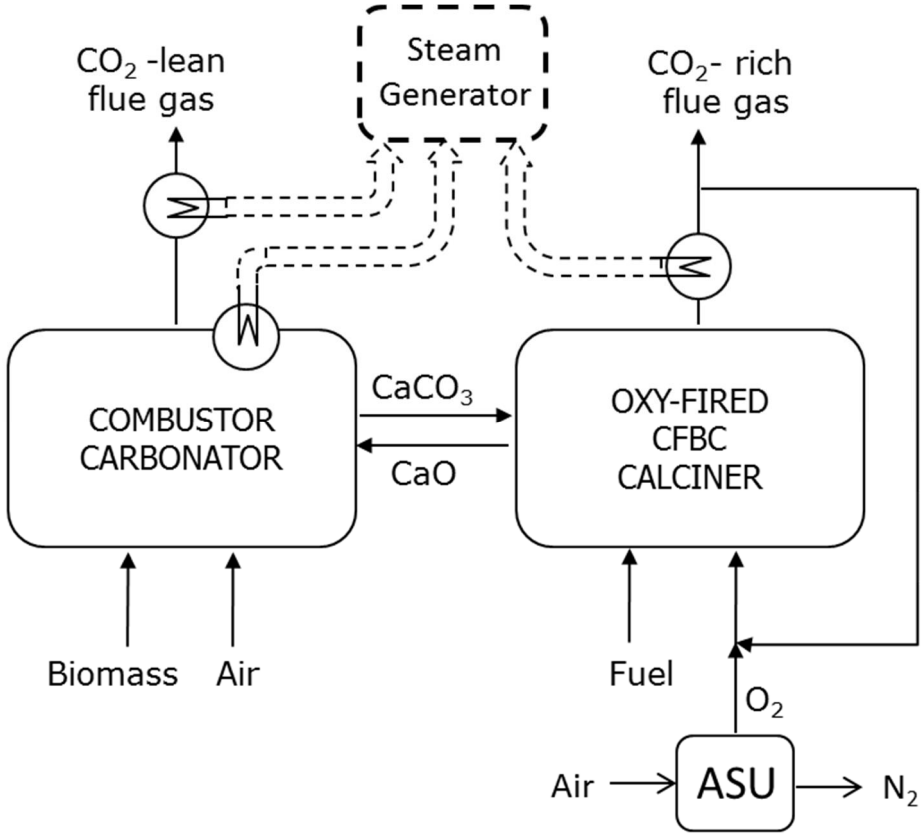

Figure 1. General scheme for the biomass combustion with in-situ CO_2 capture by CaO process.

The fundamental advantage of the system of Figure 1 respect to stand alone oxy-fired scheme is that the O_2 consumption is about 1/3 of the equivalent oxy-fired system burning the same total flow of biomass and fuel. A recent economic and process analysis of the concept of Figure 1 (Ozcan et al., 2014) has revealed the technical and economic boundary conditions for this niche application of Calcium Looping and biomass firing in power plants to be economically viable. The close similarity of each of

the main reactors in the system with commercial CFBC power plants enables an evaluation of electricity and CO_2 avoided cost (Ozcan et al., 2014) that indicates that this process achieves around 43 €/ton CO_2 avoided, only slightly lower than the cost of a stand-alone oxy-fired system burning biomass operating under comparable conditions. However, a further advantage of this system is that it can be adapted to a wider range of regulatory conditions and avoided cost can even take negative values when there are economic incentives for the both the storage of CO_2 from biomass firing and green certificate for biomass use in air fired power plants. The in-situ calcium looping option becomes more economical and more flexible to adapt to different market conditions than air-fired biomass plants and oxy-fired plants alone. This is particularly the case when the biomass plant is co-located with an oxy-fired coal power plant or a much larger post-combustion calcium looping plant supplying the CaO to the combustor carbonator (Ozcan et al., 2014).

The purpose of this work is to report experimental results from a 300 kW_{th} pilot designed, built and operated to demonstrate the viability of the process in an industrial environment and with sufficiently long duration tests (up to a week-long). The pilot is located at a 655 MW_e coal power plant of "GNF-La Robla" (León, Spain). Several series of experiments, specially focused in the demonstration of the simultaneous combustion-carbonation reactor concept, have been successfully achieved so far. The interpretation of experimental results with a simple reactor model for combustion and CO_2 capture by CaO in the combustor-carbonator are also discussed in this work to aid in future scaling up of this novel CO_2 capture concept with negative emissions.

EXPERIMENTAL

Two interconnected circulating fluidized bed reactors (combustor-carbonator and calciner) are at the core of the pilot plant used to carry out the experimental campaigns in this work. The height of both reactors is 12 m and the internal diameter is about 0.4 m. Although the process concept of Figure 1 involves O_2/CO_2 combustion in one of the reactors, the design of this pilot has been simplified to operate in air-combustion mode in both reactors. This allows to test under more controlled conditions the novel reactor in the system (the combustor-carbonator). Air is blown to both $CFBC_s$ using two fans and is introduced as primary air to the bottom of the reactors by nozzles. Only a small fraction of secondary air (about 10 vol%) comes as secondary air with the biomass feed. The solids that exit the reactors are separated by means of primary cyclones and sent through standpipes to the bubbling bed loop-seals, which are equipped with two chambers fluidized with air. The particles that abandon the loop-seals go into a dipleg where they flow by gravity towards the opposite reactor. There are also two secondary cyclones that recover very few solids

under normal operating conditions but that act as a security solid separation devices when a malfunction in the operation in the primary cyclones occurs (for example by a rupture of the gas seal in the loop-seals).

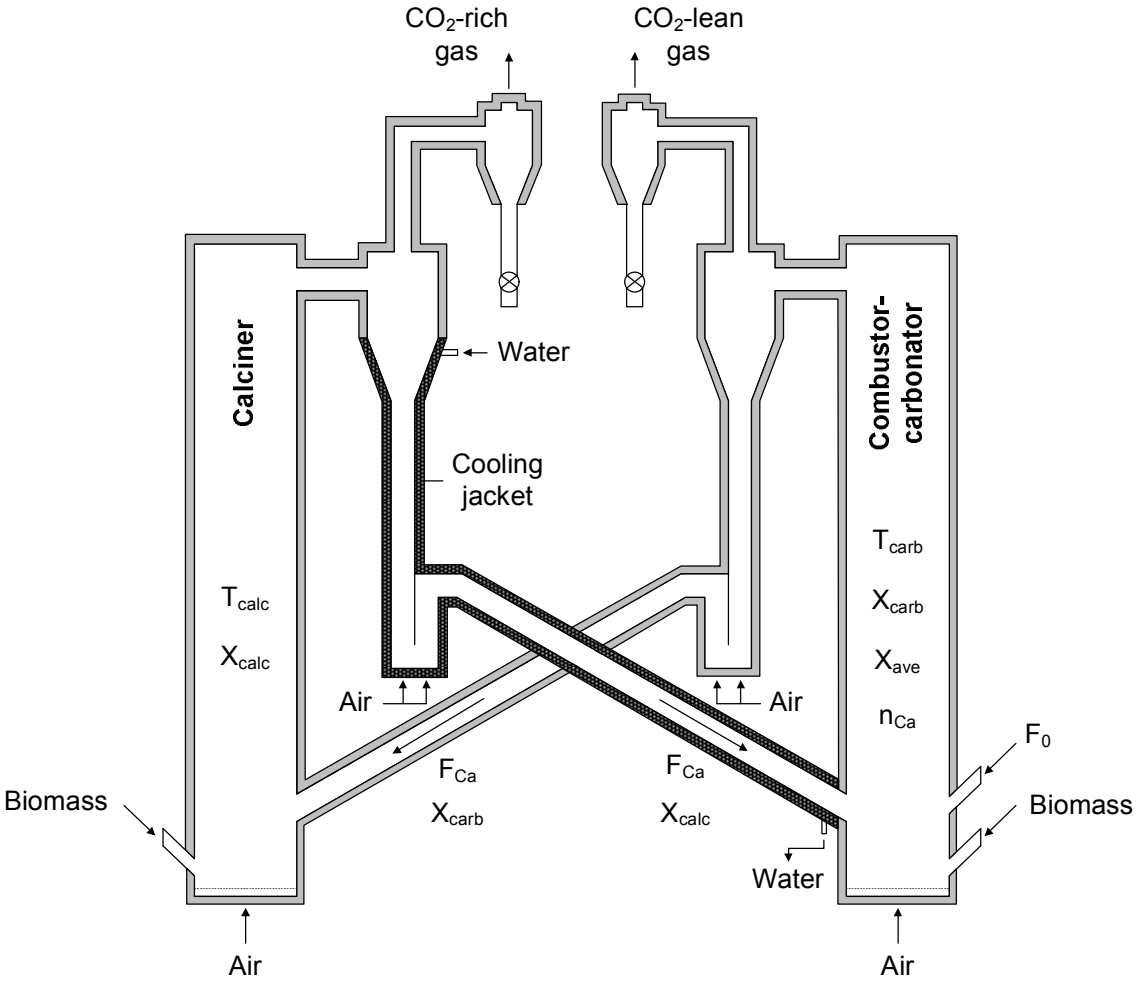

Figure 2. Scheme of "La Robla" Calcium Looping pilot plant with the main inputs and operating variables. The grey shaded area is refractory lined, the black shaded area is cooled areas through water jackets.

Both reactors are refractory lined (grey shaded area in Figure 2) to reduce heat losses and maintain the high temperatures required by the process. The same happens to the cyclone, the standpipe, the loop-seal and the dipleg that carry solids from the combustor-carbonator to the calciner, where the presence of refractory avoids excessive cooling of the particles and reduces the amount of fuel required to heat this stream up to calcination temperature. The thermal insulation of the upper part of the primary cyclone and the secondary cyclone of the calciner has been reinforced to minimize drops in temperature in such region leading to deposit formation due to carbonation of CaO particles under the richer CO_2 atmospheres abandoning the calciner.

A critical aspect in the pilot design has been the temperature control system in the combustor-carbonator. In order to balance the strong exothermic character of the combustion-carbonation reactions taking place at the bottom of the reactor, it was decided to cool down the solids entering the bottom of the combustor-carbonator and coming from the calciner. For this purpose, water jackets (black shaded area in Figure 2) were placed over the truncated-cone region of the cyclone, along the standpipe, the loop-seal and the dipleg associated to the calciner to extract heat from the solids flowing from the calciner to the combustor-carbonator. As will be shown later, this heat transfer strategy proved to be successful in sustaining the required temperatures for simultaneous combustion and carbonation in the reactor.

Biomass pellets are continuously fed into the combustor-carbonator and the calciner reactors by water-cooled screw feeders. There is also the possibility to introduce a continuous make-up flow of fresh limestone into the combustor-carbonator by means of a screw feeder. This flow contributes to maintain a stable inventory of solids, since a fraction of fine particles leave the facility either through the secondary cyclones or suspended on the gas that exits the facility through the stack. Solids can be extracted continuously during operation from the combustor-carbonator and in batches from the calciner by opening the valves located in the bottom of the reactors. There are also sampling ports at the exit of the reactors that allow the extraction of solids samples and measure solids circulation rate with isokinetic probes. These solid samples are further analysed by a C/S analyser and a thermogravimetric analyser and the results obtained are used to close the carbon balance and to provide reactivity information for model validation purposes. There are also temperature and pressure taps distributed in different locations in the facility. Zirconia oxygen probes are installed at the middle and the upper part of the combustor-carbonator and at the upper part of the calciner to acquire instant O_2 concentrations in those locations. The dry gas composition at the exit of the reactors is registered by using two gas analysers after the secondary cyclones. Both gas analysers measure continuously the CO_2, O_2 and CO content of the gas and one of them also measures the C_xH_y as a CH_4 concentration. They can be switched between reactors, so that they can both be used to characterise the gas stream generated either in the combustor-carbonator or the calciner. The CO_2 capture efficiency can be estimated from these gas concentration measurements by

$$E_{carb} = \frac{F_{CO2,comb} - F_{CO2,out}}{F_{CO2,comb}} \qquad (1)$$

where $F_{CO2,comb}$ is the CO_2 flowrate generated by combustion and estimated from an oxygen balance, using the continuous O_2 measurement at the exit of the combustor-carbonator by the oxygen probe and the analyser in order to take into account a certain split of air across the loop-seal, the flow rate of air through the reactor and the

loop-seal and the elemental analysis of the fuel fed to the reactor. The detailed procedure is described elsewhere (Abanades et al., 2011b).

In addition, it is useful to compare continuously the experimental capture efficiency, E_{carb}, with the maximum CO_2 capture allowed by the equilibrium, E_{eq} that can be estimated by:

$$E_{eq} = \frac{F_{CO2,comb} - F_{CO2,eq}}{F_{CO2,comb}} \quad (2)$$

and the $F_{CO2,eq}$ is calculated from (Barker, 1973):

$$\nu_{CO2,eq} = 4.137 \times 10^{7} e^{-20474/T} \quad (3)$$

All the experimental campaigns were carried out feeding wood pellets, whose composition and heating values are listed in Table 1. Additionally, two Spanish limestones and another one coming from Germany, which had initial mean particle diameter of 93 μm, 348 μm and 87 μm respectively, were used.

Table 1. Analysis of the biomass pellets used during the experiments (mass basis).

Proximate analysis	Moisture (%)	6.9
	Ash (%)	0.4
	Volatile (%)	84.4
	Fixed Carbon[b] (%)	8.3
Ultimate analysis[a]	C (%)	50.7
	H (%)	6.11
	N (%)	0.20
	S (%)	0.01
	O[b] (%)	42.3
	LHV (MJ/kg)	19.2
	HHV (MJ/kg)	20.4

[a] Dry basis. [b] by difference

The standard experimental procedure starts with heating the reactors and the solid beds with two propane burners until the bed temperatures are around 300 ºC and the gas lines are above 100 ºC in order to avoid effects related to water condensation. Then, biomass is fed to both reactors but the gas velocity is kept low in order to increase the temperature at the bottom of the reactors as soon as possible by limiting the solids circulation between reactors. Once the temperature at the bottom of the reactors is higher than 550 ºC, the propane burners are switched off and the biomass feed rate to the reactors is increased. When the temperature is over 650 ºC, the inlet

gas velocity as well as the biomass feed rate are increased in order to increase the solids circulation rate between the reactors and to heat up the primary loop (i.e. the primary cyclones, standpipes, loop-seals and diplegs). When the temperature at the exit of the calciner primary cyclone is around 300 ºC, the water jackets are switched on in order to prevent material stresses. At a temperature around of 700 ºC inside the reactors, the inlet gas velocity of the calciner and the biomass feed rate are adjusted in order to increase the average temperature in the calciner. Whereas the biomass feed rate and the inlet gas velocity of the combustor-carbonator are adjusted to maintain the average temperature in the reactor.

RESULTS AND DISCUSSION

The test campaigns carried out in the pilot plant involve 750 h in combustion mode of which 550 h were in combustion and in situ CO_2 capture mode. The experimental range of the main operating conditions is summarized in Table 2.

Table 2. Experimental range of the main operating conditions in the tests of La Robla pilot plant.

Combustor-Carbonator Temperature (ºC)	T_{carb}	630-720
Combustor-Carbonator average gas velocity (m/s)	u_{carb}	0.9-2.8
Combustor-Carbonator solids inventory (kg/m^2)	W	60-380
Excess O_2 concentration (vol%)	$\nu_{O2,e}$	3-12
CO_2 concentration from combustion (vol%)	$\nu_{CO2,comb}$	6-15.4
Maximum average CO_2 carrying capacity of solids	X_{ave}	0.12-0.73
Solids circulation flow rate (kg/m^{2}s)	G_s	1-5
Calciner Temperature (ºC)	T_{calc}	800-950

An example of a typical experiment in La Robla is shown in Figure 3, following the experimental procedure described above. The figure is divided in 4 intervals that are briefly summarized in the auxiliary table included in the figure. The first interval is highly dynamic and corresponds to the end of the start-up period, with an arbitrary starting point (t = 0:00 h) that marks the switching off of the propane burners and the increasing of the feeding of biomass to both reactors. During this first interval the main inlet gas velocity of the combustor-carbonator was increased in order to increase the solids circulation flow rate and heat up the full primary solid circulation loop represented in Figure 1. The limestone make-up feed was switched on and off several times during this interval in order to maintain certain solids inventory in the combustor-carbonator during this non-steady state period (Figure 3b). The CO_2 capture efficiency as well as the maximum CO_2 capture efficiency fluctuated accordingly between 22-80% and 48-88 % respectively (Figure 3c). The excess air ratio during this experiment varied to be able to maintain a certain gas velocity while

varying the biomass feed rate to sustain reactor temperatures. However, this change in O_2 concentration at the exit of the combustor-carbonator (between 7 vol% and 12vol% in this experiment) had little effect on CO_2 capture efficiencies of Figure 3c. The capture CO_2 molar flowrate varied between 0.2 and 1.8 mol/m^2s during this period (Figure 3b).

The second period in Figure 3 registers the evolution of the system after setting a certain fuel and air flows to the reactors ($Q_{bio-carb}$ = 40 kg/h, $Q_{bio-calc}$ = 76 kg/h, u_{calc} = 2.8 m/s, u_{carb}= 2.3 m/s). As a result the average calciner temperature increased from 800ºC to 860 ºC and the average combustor-carbonator varied between 650ºC and 740 ºC. During this period, there is substantial oscillation in the solids inventory as a consequence of the discontinuously fresh make-up feed (see changes in void dots in Figure 3b). The CO_2 capture molar flow rate increased from 0.9 mol/m^2s to 2.3 mol/m^2s during this period (Figure 3 b) and the CO_2 capture efficiency (defined as in equation 1) increased from 22 % to a maximum of 87 % at 7:20 h whereas the maximum capture efficiency (given by equation 2) was very close to the experimental capture efficiency as the inventory of solids in the reactor increased (period 2 of Figure 3b).

The third period in Figure 3, between 7:20 h and 10:50 h, registers the effect of an increase of the inlet gas velocity to the combustor-carbonator from 2.3 m/s to 2.7 m/s. As can be seen, the average calciner temperature and the difference between calciner temperature and combustor-carbonator temperature decreased due to the increase of solid circulation rate between reactors. The CO_2 capture molar flow rate increased to 2.7 mol/m^2s at the beginning of this period as a consequence of the rapid increased in the CaO circulation flowrate. Nonetheless, it tended to decreased to 1.6 mol/m^2s because the calcination intensity was reduced (Figure 3b) in the calciner, since the temperature droped from 860ºC to 815ºC at the end of the period, and also as a consequence of the higher temperatures found within the combustor-carbonator (Figure 3a). The experimental capture efficiency, E_{carb}, and the equilibrium efficiency, E_{eq}, decreased due to the decrease in the calcination rate linked to lower temperatures in the calciner and due to the increase in the average temperature in the combustor-carbonator.

The fourth experimental period, between 10:50 and 16:00 h, corresponds to a situation as in period 2, but with a continuous flow of limestone around 60 kg/h to sustain stable solid inventories in the combustor-carbonator at around 300 kg/m^2. As can be seen, the experimental CO_2 capture is very close to the theoretical maximum during this period for these values of solid inventory in the combustor-carbonator and a stationary state regime is achieved in these conditions that can be extended for much longer periods of time. The longest experiment in steady state conditions has lasted 100 hours in this particular pilot. The interruptions in operation or the forced

changes in the steady state operating conditions have arisen from malfunction and problems associated to the auxiliary equipment necessary in these small scale pilots (biomass feeding system interruptions, problems with the discharge of solids from the secondary cyclone, deposits of $Ca(OH)_2$ and $CaCO_3$ in the cooled parts downstream of the first cyclone, etc).

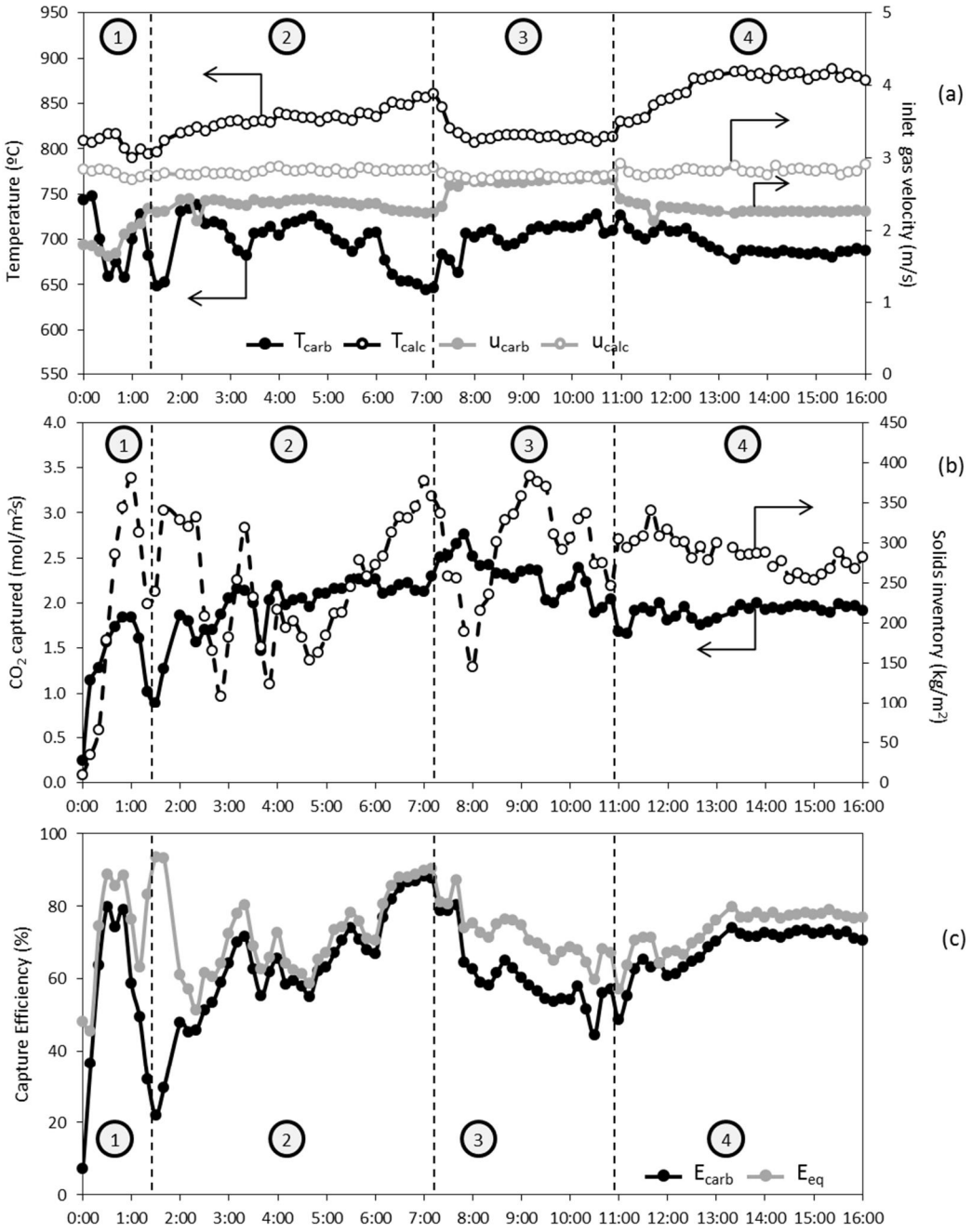

Interval	Time	Description
1	0:00 -1:40	End of the start-up period
2	1:40 - 7:20	Stable flows of biomass and air
3	7:20 - 10:50	Increase the gas velocity to combustor-carbonator
4	10:50 - 16:00	Decrease the gas velocity to combustor-carbonator with stable make-up flow of limestone

Figure 3. Example of an experimental run in La Robla pilot plant burning biomass pellets of Table 1 and feeding Omyacarb limestone of average dp of 93 μm and $CaCO_3$ content>98%.

Using the information from steady states periods (two hour duration with stable conditions as in period 4 of Figure 3), the influence of some operating variables discussed in the following paragraphs.

The effect of the solids inventory on the normalized CO_2 capture efficiency (E_{carb}/E_{eq}) is shown in the example of Figure 4a. Two parts of steady states periods with nearly identical set of operating conditions but different bed inventories are represented. The normalized carbonation efficiency is very close to 1 for the higher solids inventory (black line), which indicates that the bed is an extremely efficient reactor capturing the CO_2 generated during combustion. In contrast, despite the high value of the average CO_2 carrying capacity of the particles used in these particular experiments (X_{ave}=0.4), when solids inventory is around 100 kg/m^2 the average normalized carbonation efficiency drops down to around 0.7. In order to highlight the effect of the average CO_2 carrying capacity, Figure 4b shows the normalized CO_2 capture efficiency for other two periods at similar operating conditions. As in the previous case, due to the low solids inventory (80 kg/m^2) even at an average CO_2 carrying capacity as high as 0.4, the normalized CO_2 capture efficiency is around 0.8. When the CO_2 carrying capacity of solids decreased to 0.15, the normalized CO_2 capture efficiency decreased to around 0.65. These results emphasize the need of sufficient active solids inventory in the combustor-carbonator in order to maximize the CO_2 capture efficiency, compensating the modest average activity of the solids with increased total bed inventories.

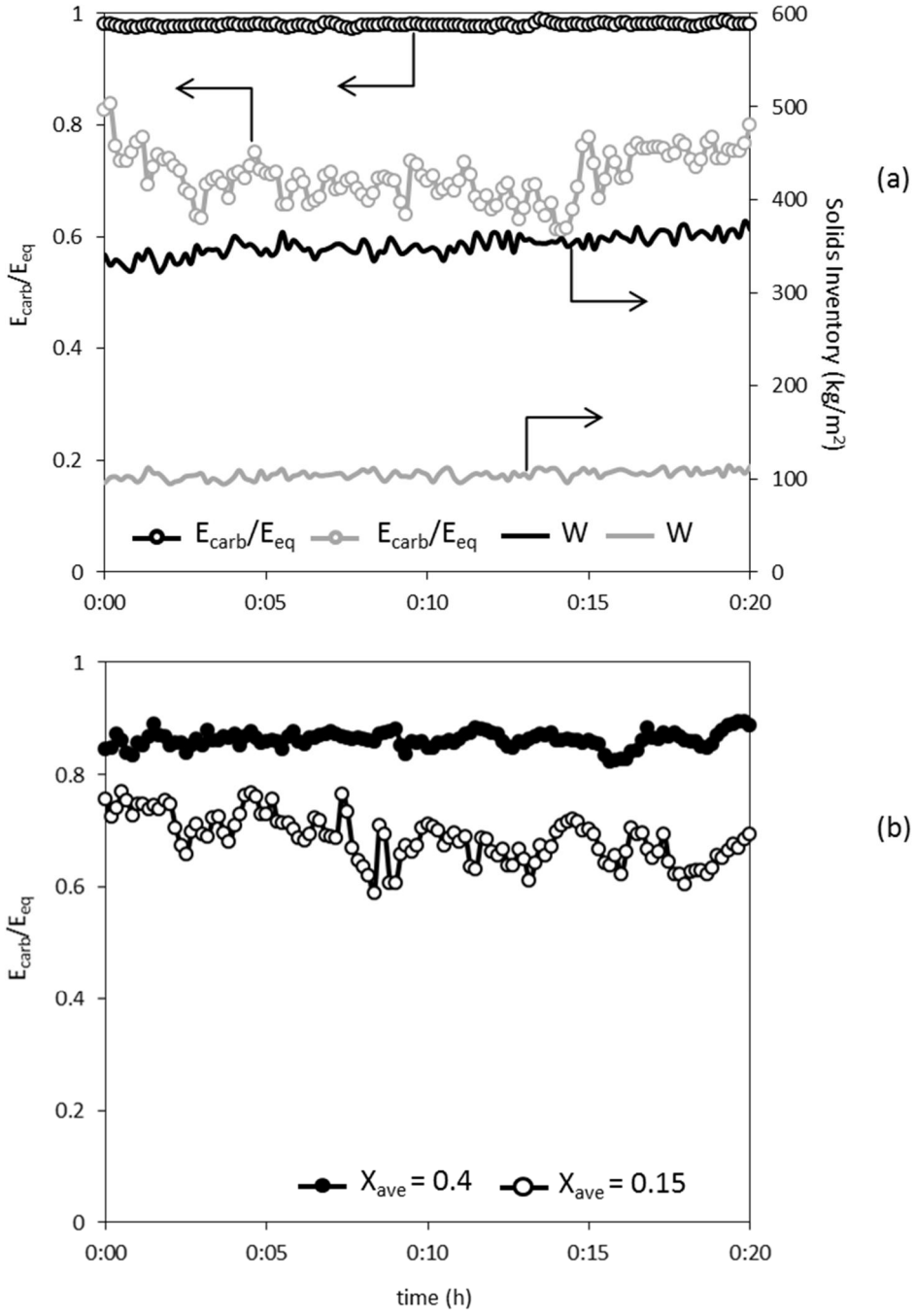

Figure 4. Effect of operating variables on the normalized CO_2 capture efficiency. (a) Effect of the solids inventory at T_{carb} = 650 ºC and inlet gas velocity of 2.4 m/s and X_{ave} = 0.4. (b) Effect of the CO_2 carrying capacity of solids at an inlet gas velocity of 1.8 m/s, T_{carb} = 700 ºC and a solids inventory of 80 kg/m^2

Figure 5 includes two examples to illustrate some effects of the average combustor-carbonator temperature on the reactor performance. Figure 5a corresponds to a rapid decrease of reactor temperature (continuous line of T_{carb}) when there is sufficient inventory of active material in the bed. In these conditions, the normalized CO_2

capture efficiency (white dots) remains almost constant and close to 1. However, as it indicated from equations (1-3), the net CO_2 capture efficiency increases when the carbonation temperature decreases as it is shown by the E_{carb} (black dots) curve. Therefore, in the absence of other limitations, the temperatures needed to achieve high CO_2 capture efficiencies in the combustor-carbonator temperature should be as close as possible to around 650º (as in other CaL systems). However, there are indications that the combustion efficiencies sharply decrease at these low temperatures. As shown in Figure 5b, the emissions of unburned gases (CO, CH_4 and other hydrocarbons) are highly sensitive temperatures below 700ºC.

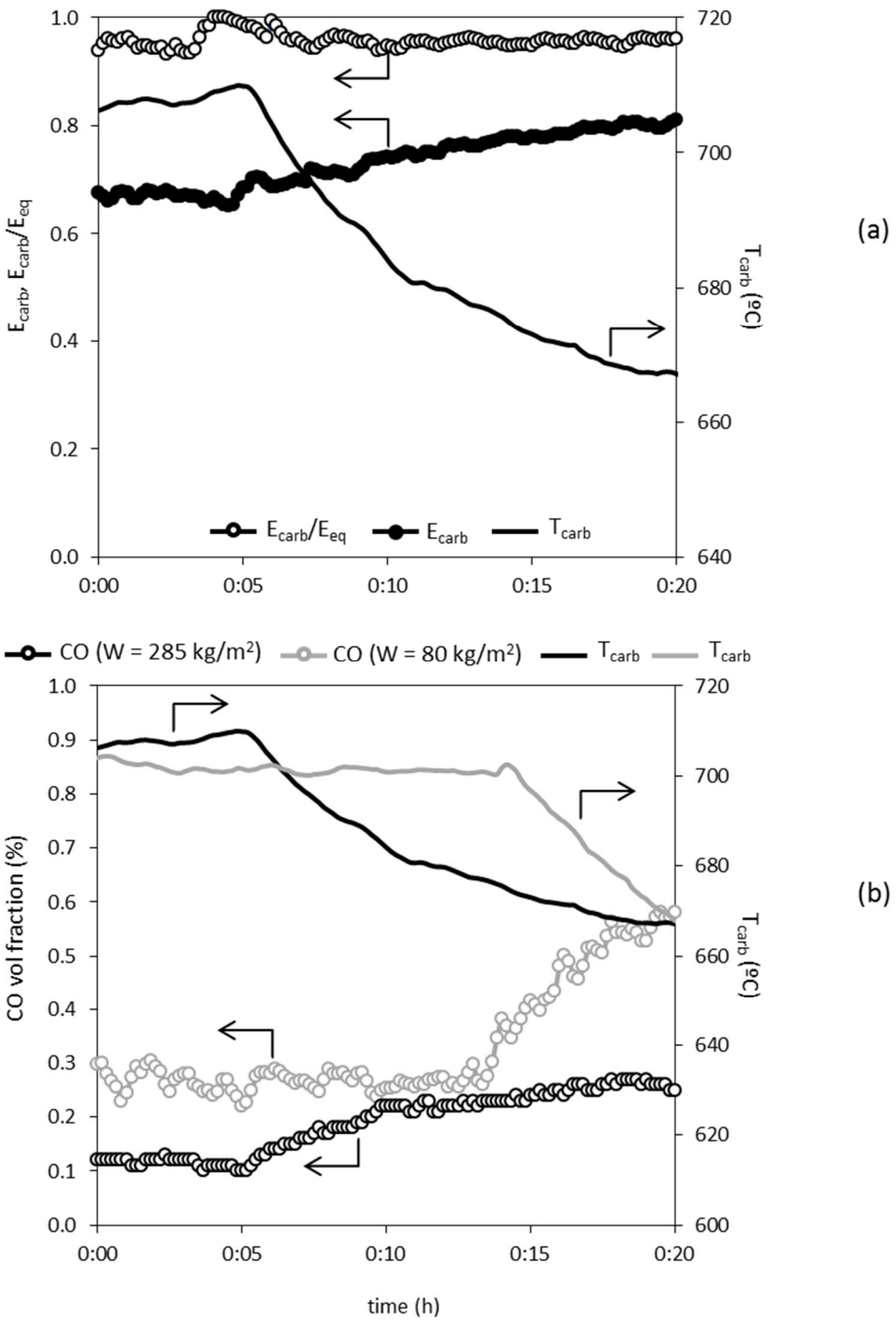

Figure 5. Effect of the average combustor-carbonator. (a) Capture efficiencies at solids inventory of 285 kg/m^2 and X_{ave} 0.3 (b) CO emissions as a function of combustor-carbonator temperature and solids inventory. (Grey symbols at solids inventory of 80 kg/m^2. Black symbols at solids inventory 285 kg/m^2). Inlet gas velocity 2.3 m/s.

During the tests carried out in this work, the CO and CH_4 concentrations were monitored continuously by the on-line gas analysers. Figure 5b illustrates the strong

dependency of combustor-carbonator temperatures with CO. As indicated in Figure 5b the bed inventory also plays a role in the emission of CO even at temperatures around 700ºC. When the solid inventory is low (W=80 kg/m^2) the average CO concentration increased from 0.3 vol% to almost 0.6 vol% (grey symbols and line). However if the solids inventory is higher (285 kg/m^2), at identical combustion conditions, the average CO goes up from 0.1 vol% to just over 0.25 vol% (black symbols and line). As discussed by (Werther et al., 2000) emissions of CO are a complex function of one or more of the following factors: a low combustion temperature, a low quality of the mixture between the air and the biomass and a low residence time of the combustible gases in the combustion zone. Other possible factor affecting CO emissions is related to different temperatures and solid loading in the primary cyclone (Leckner and Karlsson, 1993). These factors are highly dependent of the experimental set up and we do not have sufficient information in the pilot to elucidate between these effects. CH_4 emissions were below the detection limit (0.01 vol%) at normal operating conditions with temperatures over 700ºC, O_2 content over 7 vol% and bed inventories over 60 kg/m^2. The equivalent patterns of trace CH_4 emissions were much more complex and uncertain in this particular experimental set up and are omitted in this discussion. We leave as beyond the scope of this first work a detailed discussion of trace emissions. It is however obvious from the experimental results obtained so far that a narrow temperature window (around 700 ºC) has to be maintained in the combustor-carbonator to operate the concept of Figure 1 with acceptable CO_2 capture efficiencies and minimum emissions of unburned gases.

In order to facilitate a more quantitative interpretation of experimental results the closure of basic mass balances is a first. The methodology to analyse the results is only briefly explained here because it does not differ from previous studies conducted in a 30kW_{th} test rig published elsewhere (Alonso et al., 2009; Abanades et al., 2011b; Alonso et al., 2011; Charitos et al., 2011) and applied also for post-combustion CaL experiments in other test rigs (Alonso et al., 2010; Charitos et al., 2010; Charitos et al., 2011; Rodriguez et al., 2011a; Rodriguez et al., 2011b; Arias et al., 2013). The general CO_2 mass balance in the combustor carbonator at steady state conditions can be written as:

$$\begin{matrix}\mathrm{CO_2\ from\ combustion} \\ -\ \mathrm{CO_2\ in\ flue\ gas}\end{matrix} = \begin{matrix}\mathrm{net\ gain\ in\ CaCO_3\ in\ the} \\ \mathrm{circulating\ solid\ stream}\end{matrix} = \begin{matrix}\mathrm{CO_2\ reacting\ in} \\ \mathrm{the\ bed\ of} \\ \mathrm{CaO}\end{matrix} \quad (4)$$

All these terms can be estimated independently from the experimental data. The first term of equation 4 is the CO_2 captured from the combustion flue gas generated in the combustor-carbonator. This can be estimated continuously from oxygen mass balance in the combustor-carbonator and the CO_2 content in the gas stream leaving this

reactor, which allow the calculation of $F_{CO2,comb}$ and $F_{CO2,out}$, respectively (see equation 1 to estimate E_{carb}). The second term can be experimentally estimated from the measurements of circulation flow rates and the difference in carbonate contents between the samples extracted at the exit of the combustor-carbonator and at the exit of the combustor-calciner. To measure solid circulation rates we used isokinetic probes at the exit of both reactors. Moreover, using the heat balance between the water flow through the jackets to cool the circulating solids stream from calciner to combustor-carbonator (see Figure 1) it is also possible to establish a correlation for the continuous monitoring of solids circulation rates. The difference in the carbonate content of the solids samples (X_{carb} and X_{calc}) extracted from the upper part of the reactors was determined by calcination in nitrogen and/or air (to distinguish small contributions from unburned char particles). So, the first CO_2 mass balance that can be experimentally checked in the pilot unit is:

$$F_{CO2,comb} E_{carb} \approx F_{Ca} (X_{carb} - X_{calc}) \quad (5)$$

Since the make-up flow of fresh limestone is added to the combustor-carbonator, the value of X_{carb} was slightly corrected in steady state experiments to discount the contribution to X_{carb} of the fraction of fresh limestone in the circulating solids abandoning the combustor-carbonator). The application of this mass balance revealed a large difference between experiments conducted with fine limestone ($dp_0 < 100$ μm) and coarser limestones (average $dp_0 = 348$ μm). As can be seen in Figure 6, the mass balance is relatively well closed for experiments carried out with fine particles (black dots) but it is not fulfilled during the experiments with coarse limestone feed (white dots in Figure 6). We detected that the carbonate content in the combustor carbonator was much higher than usual in these experiments. It can be speculated that a certain segregation phenomena of dense and coarser limestone particles in this reactor is allowing a substantial step change in carbonate content between the average particles in the bed inventory in this reactor respect to the finer solids actually leaving the reactor and arriving to the calciner. This segregation mechanism was confirmed by measurements of particle size distributions in samples from the bottom of the reactor and samples extracted by the isokinetic probe at the top of reactor. The average particle diameter in the bottom of bed was 200 μm, between 2 and 2.5 times higher than the average particle diameter at the exit of the combustor carbonator and calciner. Since most experiments reported in this work have been conducted with fine limestones ($dp_0 < 100$ μm) no more effort has been placed in analysing the complex segregation phenomena behind the (white dot) results of Figure 6.

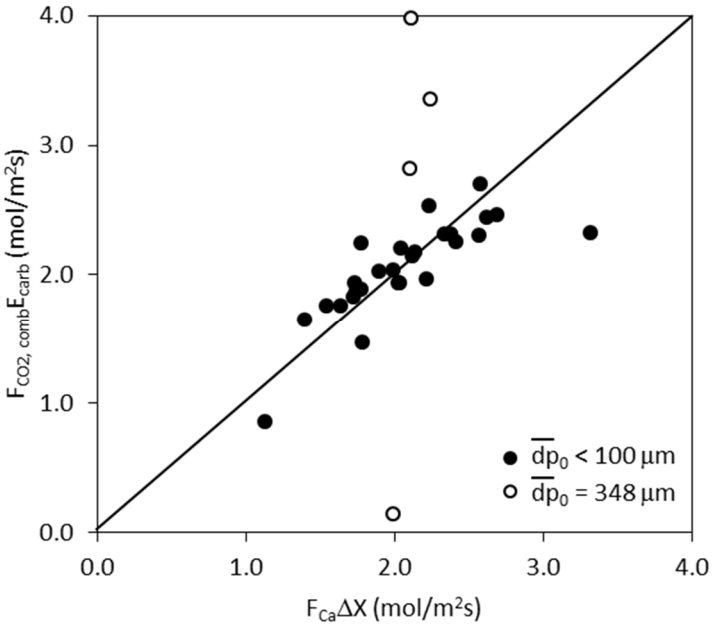

Figure 6. Comparison between the molar CO_2 removed from the combustion flue gas generated in the combustor-carbonator and the net increase of the carbonate molar flow between reactors. The second CO_2 mass balance incorporates the kinetics of the CO_2 carbonation reaction taking place in the combustor-carbonator reactor:

$$F_{CO2,comb}E_{carb} = n_{Ca,active}\left(\frac{dX}{dt}\right)_{reactor} \quad (6)$$

This equation expresses the fact that a certain inventory of active CaO particles in the combustor-carbonator is responsible of the capture of CO_2 from the flue gas by means of a certain average reaction rate of carbonation in the reactor (dX/dt). In order to attempt the closure of this mass balance, a simple carbonator model discussed in a previous work (Alonso et al., 2009) is adopted here, which assumes perfect mixing of solids and plug flow for the gas phase. Experimental data obtained in dynamic mode or in transient conditions (like those in experimental periods in 1-3 in Figure 1) or data obtained with coarse materials (segregation effects noted in Figure 6) where not considered in the fitting exercise of the model to the experiments. Only those experimental periods with fine particles (well mixed in the combustor-carbonator) and sufficient stability, represented by average values of temperature, solid inventory, average activity of the solids in the reactors, gas velocities and stable values of experimental efficiencies (E_{carb}) and CO_2 generation by combustion, were considered. In these conditions, it can be assumed that particles react at a constant rate until the maximum carrying capacity (X_{ave}) is reached and after that point the reaction rate becomes zero:

$$\left(\frac{dX}{dt}\right)_{reactor} = k_{S,ap} X_{ave} \left(M_{CO2} - M_{CO2,eq}\right)$$

$$\left(\frac{dX}{dt}\right)_{reactor} = 0 \quad \text{if} \quad X \geq X_{ave} \tag{7}$$

where $k_{S,ap}$ is the apparent reaction constant (s^{-1}).

In order to calculate the average CO_2 concentration during "in situ" combustion of biomass in the combustor-carbonator, it is further assumed that the O_2 concentration decays exponentially in the bed from the inlet O_2 concentration ($\nu_{O2,0}$) to the measured exit concentration (experimental $\nu_{O2,\ exit}$). In these conditions, the final expression for the average CO_2 concentration over the bed is as follows, (Abanades et al., 2011b):

$$\left(M_{CO2} - M_{CO2,eq}\right) = \frac{u}{h} \frac{\left(\nu_{O2,0} - \nu_{O2,e}\right)}{\left(k_{carb} - k_{comb}\right)} \left(1 - e^{-k_{comb}\frac{h}{u}}\right) - \frac{k_{comb}}{k_{carb}} \left(1 - e^{-k_{carb}\frac{h}{u}}\right) \tag{8}$$

where k_{carb} and k_{comb} are the volumetric kinetic constants associated with the carbonation and the combustion reactions, respectively.

Finally, taking into account the assumption of perfect mixing the active fraction of the solids can be defined as the fraction of particles with a residence time lower than the time needed to increase the carbonate content from X_{calc} to X_{ave}, t*.

$$n_{Ca,active} = n_{Ca} f_a = n_{Ca}\left(1 - e^{-t^*/(n_{Ca}/F_{Ca})}\right) \tag{9}$$

The characteristic carbonation time, t*, can be calculated from the measurements of X_{calc} and X_{ave} from the solids taken and using the reaction rate defined by equation 7 (Alonso et al., 2009; Charitos et al., 2011; Arias et al., 2013). By combining equations (7)-(9) into equation (6), the model is fully defined and a simple expression can be obtained:

$$F_{CO2,comb} E_{carb} = n_{Ca} f_a k_{S,ap} X_{ave} \left(M_{CO2} - M_{CO2,eq}\right) \tag{10}$$

where the average CO_2 concentration is calculated from equation 8 and k_{comb} from the exit O_2 concentration measurements (see details in Abanades et al 2011b).

The apparent reaction constant ($k_{S,ap}$) can be calculated from the experimental data as it is the only fitting parameter in equation (10), and it leads to a value of 0.095 s^{-1}, The final comparison between the CO_2 removed from the gas phase and the CO_2 reacted with the bed using this value for $k_{S,ap}$ is shown in Figure 7. The closure of the balance is reasonable as the slope of the data is close to 1. This is consistent with results reported

from smaller pilot plant and from other post-combustion systems (Abanades et al., 2011b; Alonso et al., 2011; Charitos et al., 2011; Rodriguez et al., 2011a; Rodriguez et al., 2011b; Arias et al., 2013), which provides confidence for the future scalability of the model and the data..

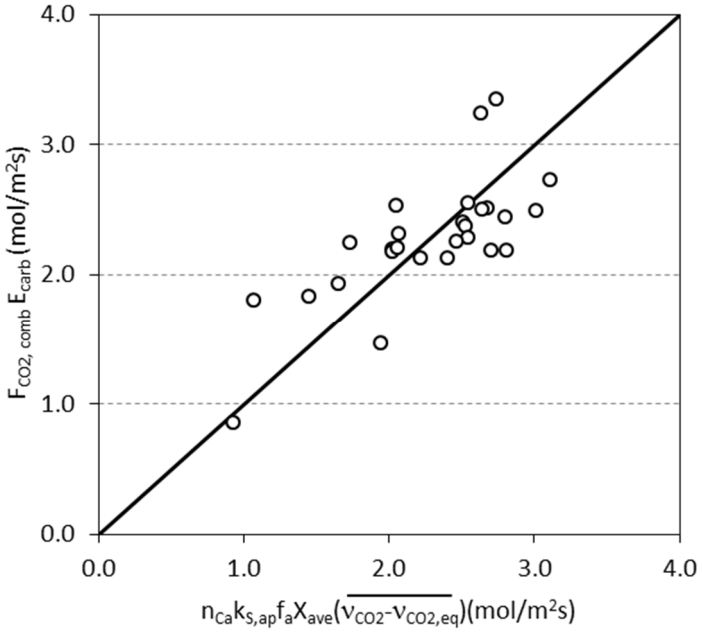

Figure 7. Closure of the mass balance between the CO_2 removed from the gas phase and CO_2 reacted in the reactor bed.

Finally, a different way of comparison between experimental data and model predictions is shown in Figure 8 using the normalized CO_2 capture efficiency is represented as a function of the active space time (τ_{active}) defined by (Charitos et al., 2011) as:

$$\tau_{active} = \frac{n_{Ca}}{F_{CO2,\,comb}} f_a X_{ave} \qquad (11)$$

where the solids inventory, the solids activity and the reaction rate are linked through the active fraction f_a. From equation (11), it can be deduced that a low X_{ave} can be compensated with high solids inventory independently of the combustion sub-model adopted to estimate the CO_2 average concentration in the bed. So, in theory, it is possible to achieve similar τ_{active} values for very different values of solids inventory and X_{ave}.

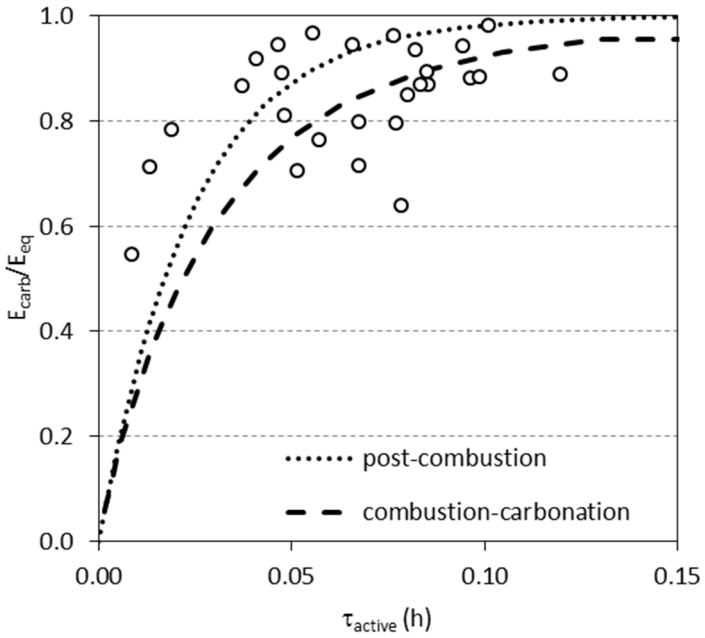

Figure 8. Normalized capture efficiency as a function of the active space time and model predictions for post-combustion and combustion-carbonation assumptions.

In the case of Figure 8, the model predictions were estimated for two different model cases: assuming that the combustion constant reaction was infinite (equivalent to a post-combustion where the flue gas resulting from the biomass combustion is all generated at the entrance of the combustor-carbonator) and assuming that the CO_2 molar flow from combustion was generating along the bed (combustion-carbonation case referred above). For this purpose, the value of the input parameters in the model were chosen on the basis of the average parameters and operating conditions found in the experimental data. As Figure 8 shows, the experimental data are mostly around both extreme model lines. In order to ensure a normalized CO_2 carbonation efficiency close to 0.9 it is necessary an active space time higher than 0.1 h. These results are an important validation of the simple model described in this work as an important tool for future design and scale-up exercises.

CONCLUSIONS

A novel biomass combustion process involving the "in situ" CO_2 capture by CaO in a circulating fluidized bed has been validated in a 300 kW_{th} pilot operated in continuous mode. The operation of the combustor-carbonator reactor supplied by a continuous flow of CaO generated in a continuous fluidized bed calciner achieved 550 h in capture mode. The experimental results confirm the need to operate in a narrow temperature window around 700ºC in the combustor-carbonator, to maximize both combustion

and CO_2 capture efficiencies. CO and CH_4 emissions are an important concern at lower temperatures and the CO_2 capture efficiency rapidly drops at higher temperatures limited by the equilibrium of CO_2 on CaO. In general, the importance of a sufficient inventory of active CaO in the combustor carbonator (by increasing the CO_2 carrying capacity of the circulating solids and/or by increasing the total solids inventory) is confirmed as a critical variable to interpret result from the twin reactor system. The closure of the carbon balance in the system (CO_2 capture in the flue gas vs net carbonate circulating from combustor carbonator to calciner) has been successful when fine solid materials are used in the experiments. However, large discrepancies have been detected in experiments conducted with large particles, probably due to segregation effects of denser and coarser particles in the reactor bed inventory.

The application of a simple model for the carbonator-combustor reactor, that assumes perfect and instant mixing of solids and plug flow for the gas phase is sufficient to approximate the experimental results with a reasonable apparent reaction constant. Active space times over 0.1 h are needed to ensure CO_2 capture efficiencies close or over 90%. The experimental results and the fitting parameters obtained in this work should be a valuable tool for scaling up of this technology.

NOTATION

E	CO_2 capture efficiency
F	Molar flow rate, mol/m^2s
F_0	Molar fresh limestone make-up, mol/m^2s
F_{Ca}	Calcium molar flow rate between reactors, mol/m^2s
f_a	Active fraction of solids
G_s	Solids circulation flow rate, kg/m^2s
h	Reaction height, m
k	Volumetric reaction constant, s^{-1}
$k_{S,ap}$	Apparent superficial carbonation reaction constant, s^{-1}
n_{Ca}	Calcium mol in the combustor-carbonator, mol/m^2
Q	Mass flow rate, kg/h
T	Temperature, ºC
u	Gas velocity, m/s
W	Solids inventory in the combustor-carbonator, kg/m2
X	Carbonate molar fraction
X_{ave}	Maximum carrying capacity

Subscripts

bio	Biomass
carb	At combustor-carbonator
calc	At calciner
comb	combustion
out	at the exit of combustor-carbonator

eq	At equilibrium conditions
O2,0	O2 at the inlet of combustor-carbonator
O2,e	O2 at the excess
Greek Letters	
ν	Volumetric fraction, (vol%)
α	Stoichiometric coefficient

ACKNOWLEGMENTS

This work was partially funded under the MENOS CO2 project (CDTI, Spanish Ministry of Economy and Competitivity). M.E. Diego acknowledges the award of a fellowship Grant under the CSIC JAE Programme, co-funded by the European Social Fund.

REFERENCES

Abanades, J.C., 2002. The maximum capture efficiency of CO_2 using a carbonation/calcination cycle of $CaO/CaCO_3$. Chem. Eng. J. 90, 303-306.

Abanades, J.C., 2013. Calcium looping for CO_2 capture in combustion systems, in: Scala, F. (Ed.), Fluidized bed technologies for near-zero emission combustion and gasification. Woodhead Publishing Limited, Cambridge, pp. 931-971.

Abanades, J.C., Alonso, M., Rodriguez, N., 2011a. Biomass Combustion with in Situ CO2 Capture with CaO. I. Process Description and Economics. Ind. Eng. Chem. Res. 50, 6972-6981.

Abanades, J.C., Alonso, M., Rodriguez, N., 2011b. Experimental validation of in situ CO2 capture with CaO during the low temperature combustion of biomass in a fluidized bed reactor. Int. J. Green. Gas. Cont. 5, 512-520.

Abanades, J.C., Alvarez, D., 2003. Conversion limits in the reaction of CO_2 with lime. Energy Fuels 17, 308-315.

Abanades, J.C., Anthony, E.J., Lu, D.Y., Salvador, C., Alvarez, D., 2004. Capture of CO_2 from combustion gases in a fluidized bed of CaO. AIChE J. 50, 1614-1622.

Alonso, M., Rodriguez, N., Gonzalez, B., Arias, B., Abanades, J.C., 2011. Biomass Combustion with in Situ CO2 Capture by CaO. II. Experimental Results. Ind. Eng. Chem. Res. 50, 6982-6989.

Alonso, M., Rodriguez, N., Gonzalez, B., Grasa, G., Murillo, R., Abanades, J.C., 2010. Carbon dioxide capture from combustion flue gases with a calcium oxide chemical loop. Experimental results and process development. Int. J. Green. Gas. Cont. 4, 167-173.

Alonso, M., Rodriguez, N., Grasa, G., Abanades, J.C., 2009. Modelling of a fluidized bed carbonator reactor to capture CO2 from a combustion flue gas. Chem. Eng. Sci. 64, 883-891.

Anthony, E.J., 2011. Ca looping technology: current status, developments and future directions. Greenhouse. Gas. Sci. Technol. 1, 36-47.

Arias, B., Diego, M.E., Abanades, J.C., Lorenzo, M., Diaz, L., Martínez, D., Alvarez, J., Sánchez-Biezma, A., 2013. Demonstration of steady state CO2 capture in a 1.7MWth calcium looping pilot. Int. J. Green. Gas. Cont. 18, 237-245.

Barker, R., 1973. Reversibility of the reaction $CaCO_3$ <———>$CaO + CO_2$. J Appl Chem Biotechnol 23, 733-742.

Blamey, J., Anthony, E.J., Wang, J., Fennell, P.S., 2010. The calcium looping cycle for large-scale CO2 capture. Prog. Energy Comb. Sci. 36, 260-279.

Boot-Handford, M.E., Abanades, J.C., Anthony, E.J., Blunt, M.J., Brandani, S., Mac Dowell, N., Fernández, J.R., Ferrari, M.C., Gross, R., Hallett, J.P., Haszeldine, R.S., Heptonstall, P., Lyngfelt, A., Makuch, Z., Mangano, E., Porter, R.T.J., Pourkashanian, M., Rochelle, G.T., Shah, N., Yao,

J.G., Fennell, P.S., 2014. Carbon capture and storage update. Energy and Environmental Science 7, 130-189.
Chang, M.H., Huang, C.M., Liu, W.H., Chen, W.C., Cheng, J.Y., Chen, W., Wen, T.W., Ouyang, S., Shen, C.H., Hsu, H.W., 2013. Design and Experimental Investigation of Calcium Looping Process for 3-kWth and 1.9-MWth Facilities. Chemical Engineering and Technology 36, 1525-1532.
Charitos, A., Hawthorne, C., Bidwe, A.R., Sivalingam, S., Schuster, A., Spliethoff, H., Scheffknecht, G., 2010. Parametric investigation of the calcium looping process for CO2 capture in a 10 kW(th) dual fluidized bed. Int. J. Green. Gas. Cont. 4, 776-784.
Charitos, A., Rodriguez, N., Hawthorne, C., Alonso, M., Zieba, M., Arias, B., Kopanakis, G., Scheffknecht, G., Abanades, J.C., 2011. Experimental Validation of the Calcium Looping CO_2 Capture Process with Two Circulating Fluidized Bed Carbonator Reactors. Ind. Eng. Chem. Res. 50, 9685-9695.
Dieter, H., Bidwe, A.R., Varela-Duelli, G., Charitos, A., Hawthorne, C., Scheffknecht, G., 2014. Development of the calcium looping CO2 capture technology from lab to pilot scale at IFK, University of Stuttgart. Fuel.
Galloy, A., Ströhle, J., Epple, B., 2011. Design and operation of a 1 mwth carbonate and chemical looping CCS test rig. VGB PowerTech 91, 64-68.
Hawthorne, C., Dieter, H., Bidwe, A.R., Schuster, A., Scheffknecht, G., Unterberger, S., Käb, M., 2010. CO2 Capture with CaO in a 200 kWth dual fluidized bed pilot plant, 10th International Conference on Greenhouse Gas Control Technologies. Energy Procedia, Amsterdam (Netherlands).
IPCC, 2014. Mitigation of Climate Change. Working group III. Contribution to the IPCC 5th Assessment Report. Summary for Policymakers, in: Edenhofer, O., Pichs-Madruga, R., Sokona, Y., Kadner, S., Minx, J., Brunner, S. (Eds.), http://www.ipcc.ch/report/ar5/wg3/.
Ishitani, H., Johansson, T.B., 1996. Energy supply mitigation options, in: Watson, R.T., Zinoyowera, M.C., Moss, R.H. (Eds.), Climate Change 1995: Impacts, Adaptations, and Mitigation of Climate Change: Scientific-Technical Analyses. Cambridge University Press, Cambridge, UK.
Koornneef, J., van Breevoort, P., Hamelinck, C., Hendriks, C., Hoogwijk, M., Koop, K., Koper, M., Dixon, T., Camps, A., 2012. Global potential for biomass and carbon dioxide capture, transport and storage up to 2050. Int. J. Green. Gas. Cont. 11, 117-132.
Leckner, B., Karlsson, M., 1993. Gaseous emissions from circulating fluidized-bed combustion of wood. Biomass Bioenergy 4, 379-389.
Obersteiner, M., Azar, C., Kauppi, P., Mollersten, K., Moreira, J., Nilsson, S., Read, P., Riahi, K., Schlamadinger, B., Yamagata, Y., Yan, J., van Ypersele, J.P., 2001. Managing climate risk. Science 294, 786-787.
Ozcan, D.S., Alonso, M., Hyungwoong, A., Abanades, J.C., Brandani, S., 2014. Process and cost analysis of a biomass power plant with in-situ calcium looping CO2 capture process. Ind. Eng. Chem. Res. D.O.I.: ie-2014-00606v.
Plötz, S., Bayrak, A., Galloy, A., Kremer, J., Orth, M., Wieczorek, M., Ströhle, J., Epple, B., 2012. Carbonate looping experiments with a 1 MWth test facility consisting of two interconnected CFBs, 21st Conference on Fluidized Bed Combustion, Naples, Italy.
Rhodes, J.S., Keith, D.W., 2008. Biomass with capture: negative emissions within social and environmental constraints: an editorial comment. Climatic Change 87, 321-328.
Rodriguez, N., Alonso, M., Abanades, J.C., 2011a. Experimental Investigation of a Circulating Fluidized-Bed Reactor to Capture CO2 with CaO. AIChE J. 57, 1356-1366.
Rodriguez, N., Alonso, M., Abanades, J.C., Charitos, A., Hawthorne, C., Scheffknecht, G., Lu, D.Y., Anthony, E.J., 2011b. Comparison of experimental results from three dual fluidized bed test facilities capturing CO2 with CaO. Energy Procedia 4, 393-401.
Saidur, R., Abdelaziz, E.A., Demirbas, A., Hossain, M.S., Mekhilef, S., 2011. A review on biomass as a fuel for boilers. Renewable and Sustainable Energy Reviews 15, 2262-2289.

Sánchez-Biezma, A., Diaz, L., López, J., Arias, B., Paniagua, J., De Zarraga, E., Alvarez, J., Abanades, J.C., 2012. La Pereda CO_2: A 1.7 MW pilot to test post-combustion CO_2 capture with CaO, 21st International Conference on Fluidized Bed Combustion. Enzo albano Editore, Naples, pp. 365-372.
Shimizu, T., Hirama, T., Hosoda, H., Kitano, K., Inagaki, M., Tejima, K., 1999. A Twin Fluid-Bed Reactor for Removal of CO_2 from Combustion Processes. Chem. Eng. Res. Des. 77, 62-68.
Ströhle, J., Junk, M., Kremer, J., Galloy, A., Epple, B., 2014. Carbonate looping experiments in a 1 MWth pilot plant and model validation. Fuel in press.
Werther, J., Saenger, M., Hartge, E.U., Ogada, T., Siagi, Z., 2000. Combustion of agricultural residues. Prog. Energy Comb. Sci. 26, 1-27.